Direct Visualization of Bragg Diffraction with a He–Ne Laser and an Ordered Suspension of Charged Microspheres

Bertrand H. Spencer and Richard N. Zare
Stanford University, Stanford, CA 94305

Diffraction is a celebrated means for determining crystal structure by X-ray, electron, and neutron scattering (*1*). Diffraction by electron, neutral, and ion scattering is also used to measure the structural ordering of surfaces and overlayers (*2*). Although it is easy to demonstrate diffraction effects with a He–Ne laser and a suitable optical mask (*3–5*), the direct visualization of diffraction on the atomic scale appears to be a forbidding task. This is owing to the Bragg diffraction condition that the wavelength of radiation or matter waves must be comparable in size to the spacings between ordered rows or planes of scatterers. However, this condition may be met for visible light by using a colloidal suspension of charged polystyrene microspheres (*6–12*). Such microspheres can be prepared as monodisperse samples with a standard deviation of the sphere diameters of less than 1%. Under conditions of low particle concentration as well as low ionic strength, the colloidal suspension crystallizes so as to minimize the Coulomb repulsion between the charged microspheres. These colloidal crystals are extremely fragile and are destroyed easily by shaking or shear motion. Their lattice spacings are comparable to the wavelength of visible light, causing them to appear iridescent, similar to opals (*13*, *14*). The sparkle of opals is caused by white light diffracting from silica particles (150–400 nm in diameter) present in a regular three-dimensional array so that light rays of different wavelengths satisfy the Bragg diffraction condition at different angles. With the use of the red light (632.8 nm) from a He–Ne laser colloidal suspensions of polystyrene microspheres can readily display Bragg diffraction, thus providing a direct visual demonstration of ordered structure in a crystal.

As X-rays have been used to measure atomic distances and rulers to measure classroom model distances, the red light of a helium–neon laser is used to measure colloidal crystal interparticle distances. Central to this process is diffractive scattering. We begin by describing the Bragg diffraction process, then present the information necessary for the preparation of ordered suspensions of polystyrene microspheres, and conclude by illustrating the use of the Bragg diffraction data to determine the spacing between planes in the colloidal crystal.

The Diffractive Scattering Process

When light of wavelength λ passes through a colloidal crystal, the scattered radiation shows a pattern of so-called Kossel lines consisting of dark or light bands in the diffusely scattered light where rays have been Bragg reflected away from or into directions corresponding to the Bragg angles for a set of crystal planes. This is readily understood (*15*) by considering the diffraction of radiation emitted by a point source inside the crystal (see Fig. 1). For a particular set of planes, denoted by the Miller indices (hkl) and spaced apart by the separation, d_{hkl}, radiation from the point P at the Bragg angle θ for a particular direction of emission will give, at each (hkl) plane, a transmitted beam T and a diffracted beam D. Here the Bragg reflection condition (for first-order scattering) causes θ and λ to be related by the condition that

$$2d_{hkl} \sin \theta = \lambda \tag{1}$$

The totality of all directions of T for which intensity has been removed by the diffraction process will be a cone of half-angle

$$\phi = \pi/2 - \theta \tag{2}$$

having an axis perpendicular to the (hkl) planes. The totality of all beams T' suffering diffraction will form a similar cone having an oppositely directed axis. The intersection of these cones with a viewing screen, such as photographic film, gives rise to a pattern of Kossel ellipses or rings. For the particular case of a spherical screen centered about the point P, the intersections of the Kossel cones with the screen are circles. From a simple geometrical measurement of the half-angle ϕ of the Kossel ring, the lattice spacing of the set of planes producing the Kossel ring is given by substitution of eq 2 into eq 1:

$$2d_{hkl} \cos \phi = \lambda \tag{3}$$

Here λ is the wavelength of the light within the colloidal

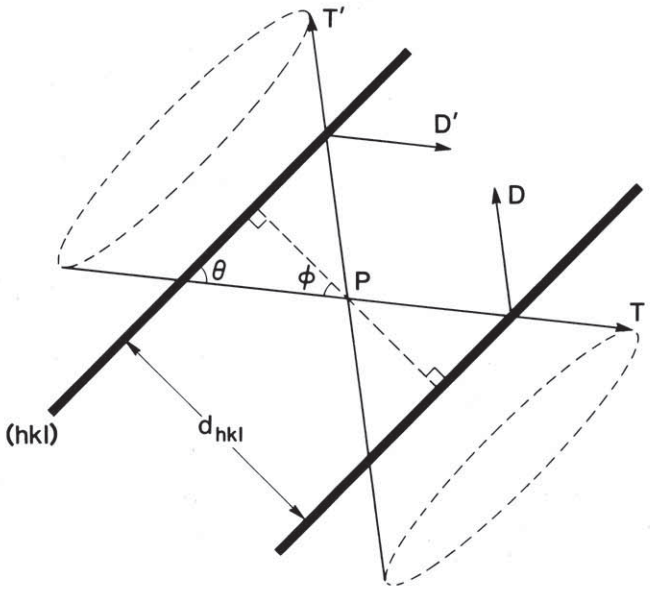

Figure 1. Diagram illustrating formation of Kossel rings caused by the diffractive scattering of divergent radiation from the scattering center P on the planes (hkl) with a separation d_{hkl}. The Kossel cone has a half angle ϕ, which is the complement of the Bragg diffraction angle θ. Here T stands for transmitted radiation and D for diffracted radiation; primed letters denote radiation initially incident on the (hkl) planes in a direction opposite to the unprimed letters.

crystal. This may be related to the vacuum wavelength λ_{vac} according to

$$\lambda = \lambda_{vac}/n \quad (4)$$

where n is the refractive index of the colloidal crystal. Hence

$$d_{hkl} = \lambda_{vac}/2n \cos \phi \quad (5)$$

From Figure 1 it is also seen that there will be a reflection from the opposite side of the crystal planes, giving a transmitted beam T' parallel to D and a diffracted beam D' parallel to T. As a result, the intensity "borrowed" from transmission by diffraction and vice versa tends to cancel. However, if absorption (extinction) is also included in this treatment, the cancellation is not complete and the Kossel lines appear with nonzero contrast (*15*, *16*).

In addition to the Kossel lines, there also appear bright spots called Laue diffraction spots. However, the Kossel rings dominate the scattering pattern for a three-dimensional colloidal crystal because of the scattering by the microspheres, whereas in X-ray diffraction from molecular crystals the reverse is normally the rule, because the scattering strength of an atom is smaller. Under conditions of X-ray scattering within the sample, as for example under bombardment by electrons or protons where X-rays are isotropically produced at some interior lattice position, Kossel rings may be clearly seen. Tixier and Wache (*17*) show how the structure of metals can be determined from such rings.

When a crystalline material is of good quality or registration, the diffraction patterns are diagnostic in that these patterns can give information about the crystal structure. An elegant but complex student experiment has been published involving the diffraction of microwaves from a "crystal" made of ¾-in. steel spheres embedded in a styrofoam matrix (*18*). By applying the Bragg diffraction condition to the scattered radiation the spacing between the steel balls can be determined. This procedure is akin to the way in which a modern-day X-ray diffractometer allows the structure of a single crystal to be "solved" (*19*).

Sample Preparation

Latex microspheres are spherical polystyrene polymers that contain ionic sulfonate groups (SO_3^-) on their surface. These spheres are usually formed in an emulsion polymerization process where the number of external sulfonate groups can be controlled. The resulting spheres have diameters ranging from 20 to 1000 nm. Because the sulfonate anions on one sphere are shielded from the sulfonate anions on another sphere by a sea of solvated ions no "crystallization" will occur. Lowering the ionic strength of the solution will reduce shielding and cause the latex spheres to order themselves in the solution as a result of electrostatic repulsions. As crystallization proceeds, one notices, visually, a change in the appearance of the solution from milky white to milky with small luminous crystal facets. Highly crystallized solutions will be quite clear with large crystalline surfaces up to several centimeters high. The type of crystal produced is dependent on the volume fraction of the latex and the ionic strength of the medium (*20*). The extent of the surface charge on the particles also plays a role in this dependence. Figure 2, taken from Monovoukas and Gast (*20*), shows a phase diagram where selection of appropriate parameters of ion concentration and volume fraction will give either a face centered cubic lattice (FCC), a body centered cubic lattice (BCC) or a disordered phase. Because the BCC form is favored energetically at lower latex concentrations, a fairly large surface charge and a highly deionized solution is required to stabilize the BCC lattice. Upon initiation, however, the BCC form will crystallize faster than the FCC form. Occasionally the two forms can coexist in solution, giving complicated diffraction patterns.

The following experimental procedure was employed in making colloidal crystal suspensions suitable for Bragg diffraction studies. Probably the most demanding part of observing Bragg diffraction from a colloidal suspension of latex microspheres is ensuring the proper crystallization of the latter. Our experience is that the major difficulty is lowering sufficiently the ionic strength of both the water and the commercial latex sphere samples used in preparing this suspension.

Regeneration of Ion Exchange Resin

Newly purchased ion exchange resins need not be regenerated. Biorad AG 501–X8(D) resin was regenerated by separating the cationic and anionic particles by sedimentation in a large beaker of water. The lower cationic resin was thoroughly soaked with 10% HCl and then washed with distilled water in a Buchner funnel. Likewise, the upper anionic resin was thoroughly soaked with 10% NaOH and then washed with distilled water. The conductivity of the wash water from each resin should be about 0.20 μS (1S = 1 ohm^{-1}). Following removal of all wash water the cationic and anionic resin particles were remixed with fresh water in a beaker and immediately collected in a Buchner funnel. The final resin was amber-green, the green particles being anionic, and appeared well mixed.

Dialysis of Latex

2.0 mL of 91 nm Duke latex particles (Lot 7009, 10% solids) were placed in preboiled dialysis tubing, the ends sealed, and the tubing then suspended in deionized water. The conductivity decreased over the course of five days to give a steady reading about equal to the conductivity of the deionized water. A few changes of the dialysis water were required through this time period. The final volume of solution in the dialysis tubing was about 8 mL, which was withdrawn from the tubing and stored in a plastic vial. The percent solids in the latex was determined to be 2.5% by evaporation and weighing.

Preparation of Thin Cells

Five thin cells were assembled consisting of two pieces of 2- × 2- × ¼-in. Plexiglas separated by a 0.03-in. Teflon sheet with a 1 × ½-in. rectangle cut out of it at its top. This rectangle became the sample container. Six holes were drilled in the assembly adjacent to the rectangular cut-out and the sandwich was tightened together by 6 machine screws, nuts, and washers.

An alternative sample holder that allows visualization of a central Kossel ring is a commercial 3- × 7- × 48-mm quartz cell (Wale Apparatus Co., Hellertown, PA).

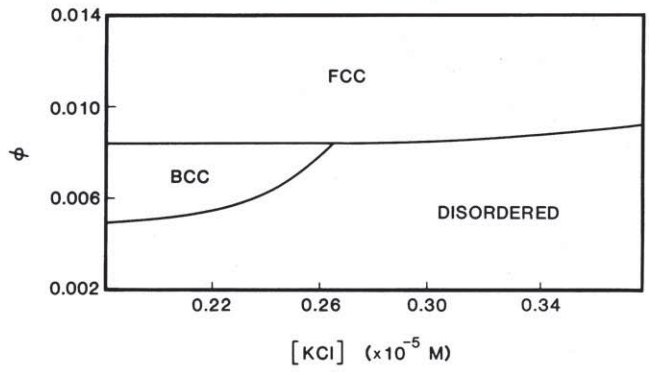

Figure 2. Phase diagram for 91-nm latex microspheres suspended in water at low ion strength as a function of volume fraction ϕ and KCl concentration, reproduced with permission from Ref. 20.

Preparation of Latex Crystals

Drops of 2.5% latex solution were added to each of five 1.0 cm^2 polystyrene cuvettes in the following amounts: 40 drops, 30 drops, 20 drops, 10 drops, and 5 drops. The total volumes were adjusted to 40 drops with deionized water. To each of the five solutions, a dozen beads of low conductivity mixed bed resin (water tested at 0.20 μS) were added to exchange residual ions in solution, and the solutions remixed. From each of the cuvettes, liquid was withdrawn and transferred to one of five thin cells to fill the void volume. Again, a dozen beads were added and the top of the thin cell was sealed with parafilm tape. At this point there were five cuvettes and five corresponding thin cells. All solutions were set aside to crystallize. Within 10 days crystals suitable for study filled the containers. Care was taken to move the samples as little as possible because the crystals are destroyed by agitation. Partial reannealing does occur on standing. The crystals can be stored for many weeks depending on the permeability of the container and on the rate at which ions are leached from the container walls.

Bragg Diffraction from Latex Crystals

Figure 3 shows an apparatus useful for examining Bragg diffraction patterns from the latex crystals in thin cells. The thin cell was connected to a translator boom by means of a connector rod. It was important to suspend the thin cell in a water bath to match approximately indices of refraction of the latex, plexiglass and surrounding medium to minimize scattering and refraction of light. A suitable *xyz* translator allowed sample movement in three dimensions. Once the laser beam was properly positioned and focused using a 31 mm plano-convex lens attached to the side of the water tank by small pieces of tape, ring-shaped shadows were visible on a paper screen covering the outside of the water bath. Some searching for the cleanest pattern was required. The use of more than one sample was frequently necessary to produce a high-quality pattern. However, it was easy to get a central dark ring. Once this was done, the distance from the sample to the screen and the diameter of the dark ring were recorded.

When the colloidal crystals were of sufficient quality, a bright halo-shaped ring as well as a dark ring in the forward scattered direction were observed. In this case, a water bath and crystallizing dish were not necessary but all of the other procedures were the same. Such behavior was only observed for thin cells where a single crystal spanned the width of the cell.

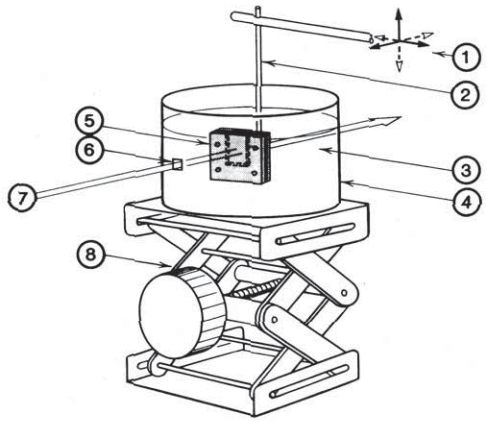

Figure 3. Apparatus for holding thin cell samples of polystyrene microspheres for viewing diffraction effects: 1 = *xyz* translator; 2 = connecting rod; 3 = crystallizing disk, 7 cm high by 13 cm in diameter; 4 = viewing screen on outside of 3; 5 = thin cell; 6 = converging lens 31 mm focal length; 7 = laser beam; and 8 = labjack.

Results

Figure 4 shows a diffraction pattern seen for 91 nm particles with a volume fraction of 0.0098, corresponding to approximately 25 × 10 (*12*) particles per milliliter. Inspection shows a central dark Kossel ring with portions of 4 other Kossel rings, one at each corner.

Light propagating through the colloidal crystal will encounter many different sets of lattice planes ($h'k'l'$). The number of Kossel rings is roughly inversely proportional to the density of the sample and can be as high as 5000 for dilute samples (*14*). Fortunately, only a few values of the Miller indices give pronounced rings at any given wavelength (*12*). In addition, the contrast of the rings decreases with increasing values of $(h^2 + k^2 + l^2)$, thereby effectively eliminating rings for larger values of (hkl). In Figure 4 the pattern of rings with nearly four-fold symmetry about the central Kossel ring indicates a BCC crystal system. Pieranski et al. (*11*) have generated a similar pattern both theoretically and experimentally for the (110) plane, albeit at the somewhat higher concentration of 60 × 10 (*12*) particles per ml. As the concentration was lowered, the rings grew in size and became tangent and the central ring disappeared. However, the four-fold symmetry was preserved for modest dilution. Monovoukas and Gast (*20*) have seen four-fold symmetry with a central ring for BCC crystals at lower concentrations. The angular separation, ϕ, of the axes of sets of Kossel cones can be fit to sets of Miller indices, (hkl), that will establish the indices of each ring and thereby determine the structure of the crystal (*12*). For BCC crystals, the (100) and (210) planes do not exist and therefore their first-order Kossel diffraction rings will be missing. Based on the four-fold symmetry of our pattern, we consider the (110) plane to be parallel to the Plexiglas face of our cell.

For a BCC crystal, the interparticle separation d is related to the separation d_{hkl} between the (hkl) planes by the equation

$$d = \frac{1}{2} d_{hkl}[3(h^2 + k^2 + l^2)]^{1/2} \qquad (6)$$

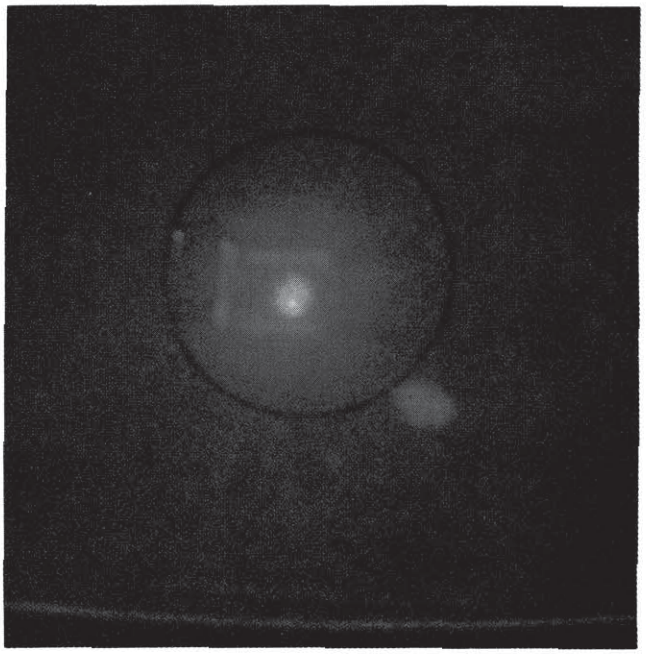

Figure 4. Photograph of the backscattered Kossel ring pattern from a BCC colloidal crystal of polystyrene spheres, 91 nm in diameter, and 0.0098 volume fraction, irradiated by the 632.8 nm light from a He–Ne laser. Shown are a central ring from the (110) plane and portions of four peripheral rings from other planes.

Thus for the (110) planes, $d = (\sqrt{6}/2)d_{110}$. We measured a half-angle $\phi = 29.2°$ for the central Kossel ring. Use of eqs 5 and 6 shows that $d_{110} = 270$ nm and $d = 330$ nm, using a value of the refractive index of $n = 1.34$ for the sample (*12*). Hence the three equal lengths of the unit cell are 380 nm.

Colloidal crystals are readily compressed, even by the Earth's gravitational field acting on a vertical column of sample only a few centimeters high! This is readily observed by varying the position that the laser beam strikes a single crystal in the vertical column and observing the size of the central Kossel ring. It is found that the size of the central Kossel ring increases linearly with increasing column height, corresponding to a uniform decrease in the lattice spacing from top to bottom in a single crystal. Indeed, a systematic investigation allows the bulk modulus (reciprocal of the isothermal compressibility) of the crystal to be determined (*12, 21*). An interesting variation is to prepare the colloidal crystals in heavy water (D_2O), rather than normal water (H_2O). Whereas the latex microspheres sink in H_2O, they float in D_2O. Consequently, the lattice of the colloidal crystal in D_2O is found to be compressed at the top of the column, whereas the opposite behavior occurs in H_2O (*21*). This confirms that the change of the Kossel ring size with column height is caused by gravitational compression, rather than some other gradient.

Conclusion

Bragg diffraction from colloidal crystals proves to be an excellent teaching tool. With relatively modest equipment and lab skills, diffraction patterns can be produced using a He–Ne laser as a coherent light source from ordered arrays of synthetic, submicron particles. This demonstration of optical Bragg diffraction from colloidal crystals gives the student an in-depth understanding of what ordered structure is and how it can be probed by diffraction techniques. At the same time, the student develops an appreciation for molecular structure at dimensions that are too small to be directly visualized.

Acknowledgment

We thank Y. Monovoukas for help in preparing crystallized colloidal suspensions and in interpreting their diffraction patterns. This work is supported by the National Science Foundation under NSF MDR 87–51200 and NSF MDR 89-54662.

Literature Cited

1. Busch, D. H.; Shull, H.; Conley, R. T. *Chemistry;* Allyn and Bacon: Boston, 1978; McQuarrie, D. A.; Rock, P. A. *General Chemistry;* Freeman: New York, 1984.
2. Zangwill, A. *Physics at Surfaces;* Cambridge University Press: Cambridge, 1988.
3. Morrison, J. D.; Driscoll, J. A. *J. Chem. Educ.* **1972,** *49,* 558.
4. Garn, P. D. *J. Chem. Educ.* **1973,** *50,* 294.
5. Brisse, F.; Sundararajan, P. R. *J. Chem. Educ.* **1975,** *52,* 414–415.
6. Luck, W.; Klier, M.; Weslau, H. *Ber. Bunseng. Phys. Chem.* **1963,** *67,* 75–83.
7. Hiltner, P. A.; Krieger, I. M. *J. Phys. Chem.* **1969,** *73,* 2386–2391.
8. Williams, R.; Crandall, R. S. *Phys. Lett.* **1974,** *48A,* 225–226.
9. Clark, N. A.; Hurd, A. J.; Ackerman, B. J. *Nature* **1979,** *281,* 57–60.
10. Dubois–Violette, E.; Pieranski, P.; Rothen, F.; Strzelecki, L. *J. Physique* **1980,** *41,* 369–376.
11. Pieranski, P.; Dubois–Violette, E.; Rothen, F.; Strzelecki, L. *J. Physique* **1981,** *42,* 53–60.
12. Carlson, R. J.; Asher, S. A. *App. Spectrosc.* **1984,** *38,* 297–304.
13. Sanders, J. V. *Nature* **1964,** *204,* 1151–1153.
14. Pieranski, P. *Contemp. Physics* **1983,** *24,* 25–73.
15. Cowley, J. M. *Diffraction Physics;* North-Holland: Amsterdam, 1981; Chapter 14, pp 309–327.
16. Rundquist, P. A; Photinos, P.; Jagannathan, S.; Asher, S. A. *J. Chem. Phys.* **1989,** *91,* 4932–4941.
17. Tixier, R.; Wache, C. *J. Appl. Cryst.* **1970,** *3,* 466–485.
18. PASCO Scientific Instrument Co., 10101 Foothills Blvd., Roseville, CA 95678, Publication WA–9314, *Microwave Optics Manual,* 1986.
19. Moore, W. J. *Physical Chemistry;* Prentice–Hall: New York, 1955, p 378.
20. Monovoukas, Y.; Gast, A. *J. Colloid and Int. Sci.* **1989,** *128,* 533–548.
21. Crandall, R. S.; Williams, R. *Science* **1977,** *198,* 293–295.